

## Supplementary Material for

# Tailoring light on three-dimensional photonic chips: a platform for versatile OAM mode optical interconnects

Jue Wang,<sup>a,b,+</sup> Chengkun Cai,<sup>a,b,+</sup> Feng Cui,<sup>a,b</sup> Min Yang,<sup>a,b</sup> Yize Liang,<sup>a,b</sup> and Jian Wang<sup>a,b,\*</sup>

<sup>a</sup>Huazhong University of Science and Technology, Wuhan National Laboratory for Optoelectronics and School of Optical and Electronic Information, Wuhan, China

<sup>b</sup>Optics Valley Laboratory, Wuhan, China

+These authors contributed equally to this work. \*Address all correspondence to Jian Wang, [jwang@hust.edu.cn](mailto:jwang@hust.edu.cn)

## Supplementary Note 1

### Fabrication of Mach-Zehnder interferometer (MZI)

The first-order mode ( $TE_{10}$ ) can be converted via an MZI, as depicted in Fig. 2(a) in the main text. The fabrication of MZI is realized by repeatedly scanning one arm, which brings a higher refractive index than the other one (estimated as higher as  $1 \times 10^{-3}$ ). This process called secondary processing adds a phase shift in the waveguide. In practice, we first fabricate the MZI with identical arms. Then, the secondary processing with different lengths (optical paths) related to different phase shifts is conducted in one arm. Figure S1 plots the left-lobe ratio (the ratio of the intensity integral of the left lobe to the total intensity integral) as a function of the secondary processing length. When the length is 0.7 mm, the left-lobe ratio is around 0.5, corresponding to an ideal  $TE_{10}$  mode.

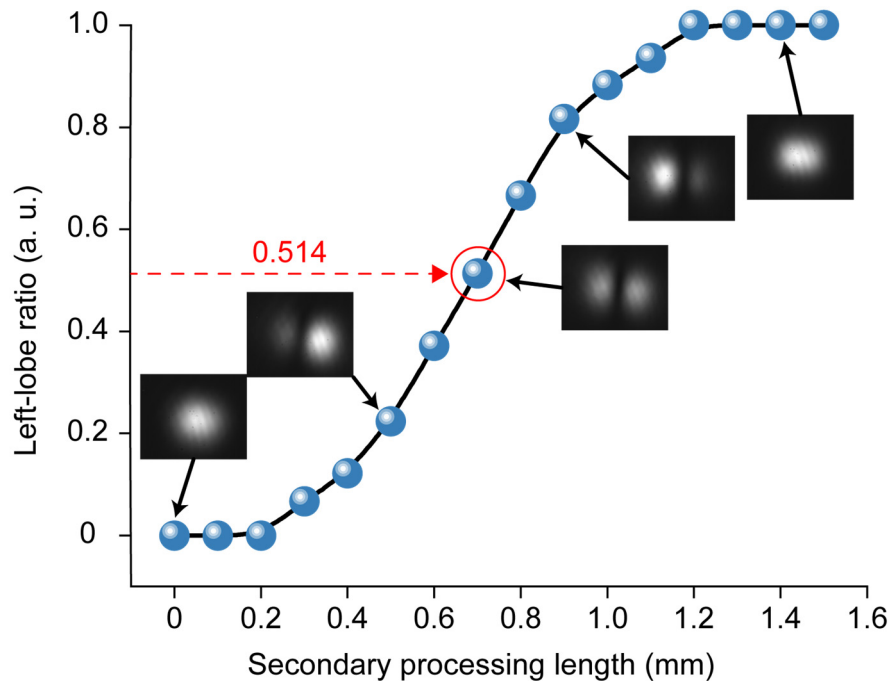


Fig. S1 The curve of the left-lobe ratio as a function of the secondary processing length.

## Supplementary Note 2

### Numerical analysis of trench waveguide for OAM mode generation

By choosing the proper trench width ( $w_1$ ) and trench height ( $h_1$ ), the higher-order eigenmodes can rotate a degree, resulting in anti-diagonal and diagonal distribution, as depicted in Fig. S2(a). We calculate the normalized overlap integrals of  $TE_{10}$  mode and anti-diagonal mode, as well as  $TE_{10}$  mode and diagonal mode, at different  $w_1$  and  $h_1$ . The normalized overlap integral is defined as

$$P = \frac{|\int E_p^* E_i dx dy|^2}{\int |E_p|^2 dx dy \int |E_i|^2 dx dy}, \quad (1)$$

where  $E_p$  and  $E_i$  are the field distribution of two modes for calculating the normalized overlap integral. The results are plotted in Fig. S2(b) and (c), respectively. It is found that when  $w_1$  and  $h_1$  are 3 and 9  $\mu\text{m}$ , the overlap ratios for two eigenmodes (anti-diagonal and diagonal modes) with  $TE_{10}$  mode are both close to 0.5.

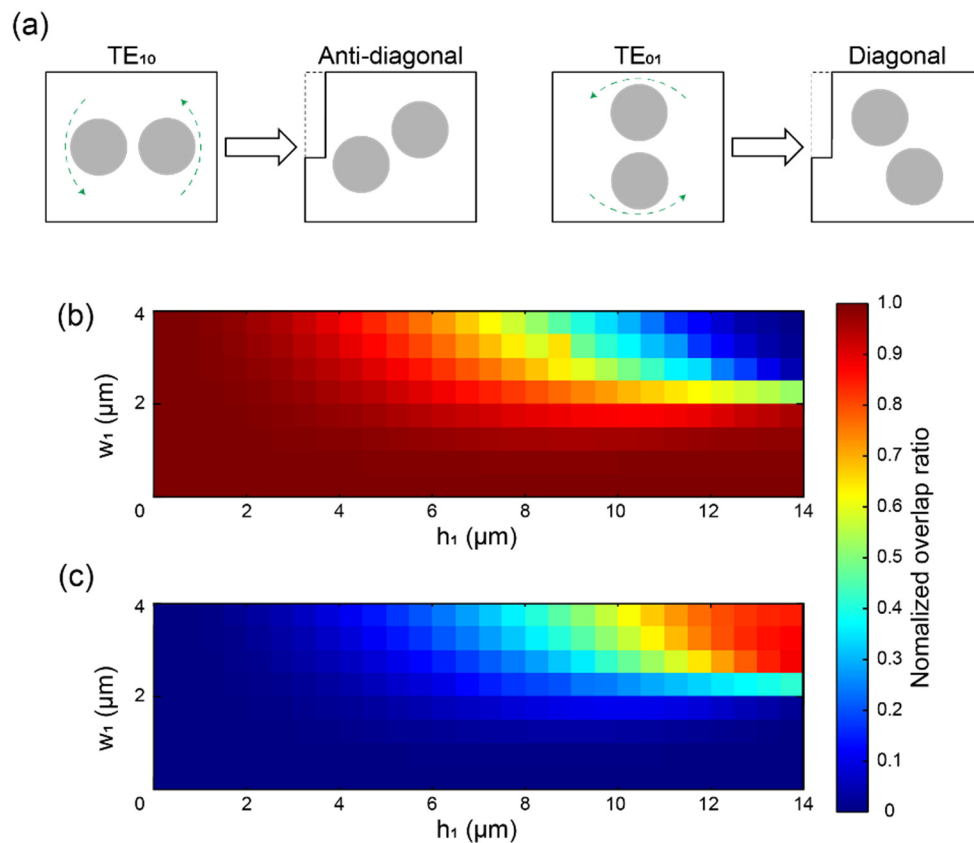


**Fig. S2 Numerical analysis of trench waveguide for OAM generation.** (a) Illustration of mode rotation for  $TE_{10}$  and  $TE_{01}$ . (b) Normalized overlap integral of  $TE_{10}$  mode and anti-diagonal mode at different trench width  $w_1$  and height  $h_1$ . (c) Normalized overlap integral of  $TE_{10}$  mode and diagonal mode at different trench width  $w_1$  and height  $h_1$ .

## Supplementary Note 3

### Mode purity for OAM mode generation

In order to characterize the mode quality of the generated OAM modes, we calculate the OAM spectra of output OAM modes. The experimental results for OAM mode generation with different trench locations are shown in Fig. S3(a)-(d), which correspond to Fig. 2(d) in the main text. We first measure their tilt interferograms as depicted in the first row of Fig. S3. Then, their actual phase distributions are reconstructed (see in the second row) using the off-axis digital holography technique. Their OAM spectra are also calculated, showing a high mode purity, as can be seen in the third row.

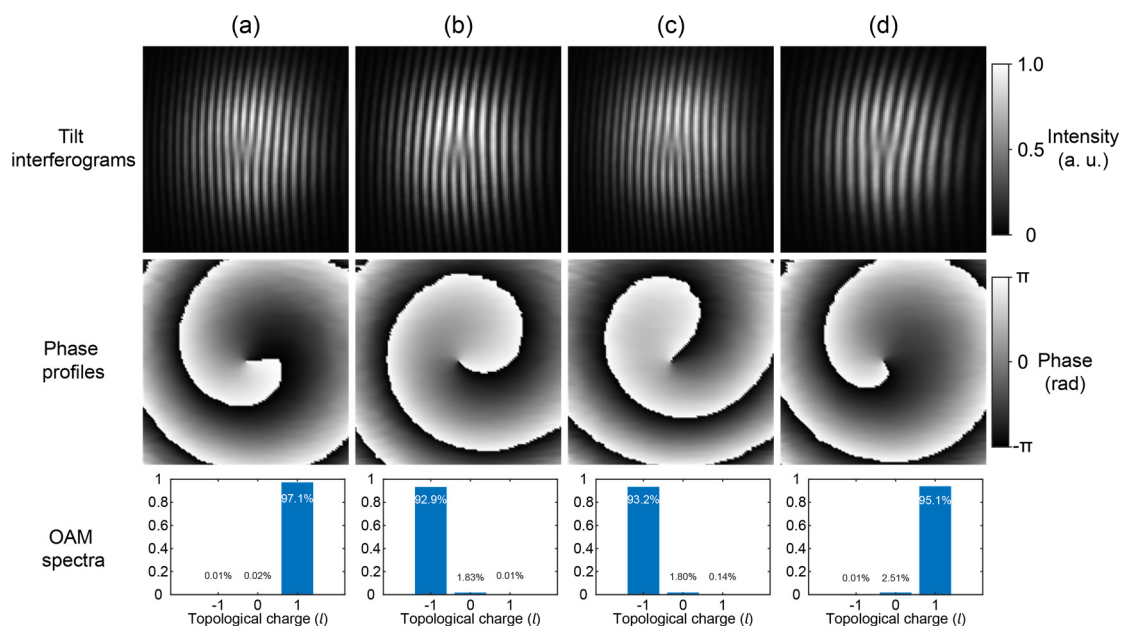


**Fig. S3** Experimental results of OAM mode generator with different trench locations. Measured tilt interferograms (the first row), retrieved phase profiles (the second row), and calculated OAM spectra with phase purities (the third row). (a)-(d) OAM mode generation with different trench locations corresponding to Fig. 2(d) in the main text.

## Supplementary Note 4

### Numerical analysis of trench waveguide for OAM mode multiplexing

We simulate mode purity of output OAM mode, calculated by normalized overlap integrals of the generated OAM mode in the trench waveguide and ideal OAM mode synthesized in the rectangle waveguide, at different trench width ( $w_2$ ) and height ( $h_2$ ), which is plotted in Fig. S4(a). When  $w_2$  and  $h_2$  are smaller than  $4.5 \mu\text{m}$ , the mode purity is more than 0.95. Figure S4(b) plots the simulated effective index difference between  $\text{TE}_{10}$  and  $\text{TE}_{01}$  at different  $w_2$  and  $h_2$ . In order to achieve a trench waveguide length with no more than 4 mm, the effective index difference should be larger than  $1 \times 10^{-4}$ , which relates to  $w_2$  and  $h_2$  larger than  $2 \mu\text{m}$ .

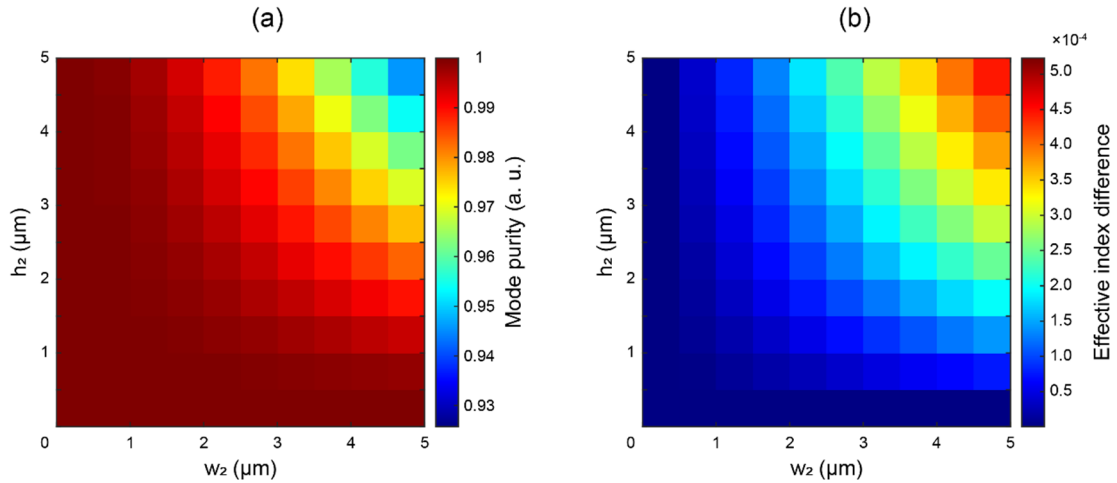


**Fig. S4 Numerical analysis of trench waveguide for OAM mode multiplexing.** (a) OAM mode purity and (b) effective index difference between  $TE_{10}$  and  $TE_{01}$  as functions of trench width  $w_2$  and height  $h_2$ .

## Supplementary Note 5

### Mode purity of OAM mode multiplexer

The quality of OAM modes generated by the OAM mode multiplexer is characterized by calculating the OAM spectra. We measure output OAM modes for input from port 1 and port 2 with trench lengths of 1.25 and 3.75 mm, as depicted in Fig. S5(a)-(d), respectively. The tilt interferograms of output OAM modes are measured, as shown in the first row of Fig. S5. Their actual phase profiles are retrieved, as depicted in the second row of Fig. S5. The OAM spectra plotted in the third row show that their phase purities are above 92%.

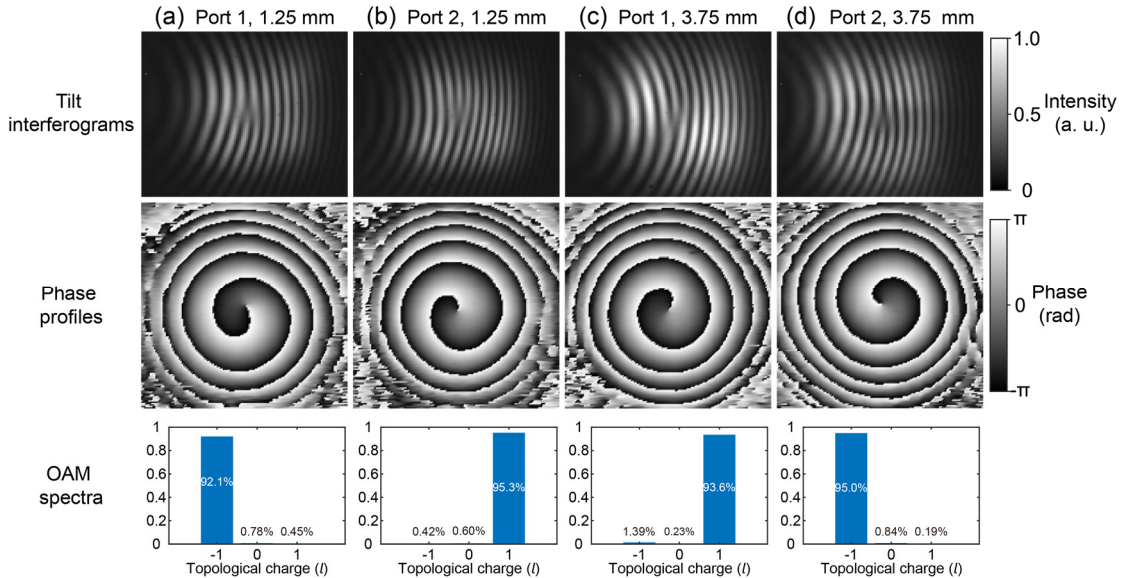


**Fig. S5 Experimental results of OAM mode multiplexers.** (a)-(d) Output OAM modes for input from (a)(c) port 1 and (b)(d) port 2 with trench lengths of (a)(b) 1.25 and (c)(d) 3.75 mm. Measured tilt interferograms (the first row), retrieved phase profiles (the second row), and calculated OAM spectra (the third row) for OAM mode multiplexers.

## **Supplementary Note 6**

### **The procedure of chip packaging**

For the chip packaging, several procedures are adopted. Firstly, the chip is glued on an aid substrate. Then we adjust the single-mode fiber (SMF) and chip, mounted on 6-axis stages, to the perfectly coupled position by observing the output profiles. Using the UV optical adhesive (Norland), the immobilization of the chip-fiber connection is achieved. We also make several fiber mounts via a 3D printer. These fiber mounts are stuck on an aid substrate. The SMFs are attached to the fiber mounts using the adhesive to make the chip-fiber connection more stable.